ANTIOXIDANTS & REDOX SIGNALING
Volume 20, Number 10, 2014

DOI: 10.1089/ars.2013.5437

ORIGINAL RESEARCH COMMUNICATION

Fus1/Tusc2 Is a Novel Regulator of Mitochondrial Calcium Handling, Ca^{2+}-Coupled Mitochondrial Processes, and Ca^{2+}-Dependent NFAT and NF-κB Pathways in $CD4^+$ T Cells

Roman Uzhachenko,[1] Sergey V. Ivanov,[2] Wendell G. Yarbrough,[2–4] Anil Shanker,[1] Ruslan Medzhitov,[5] and Alla V. Ivanova[2]

Abstract

Aims: Fus1 has been established as mitochondrial tumor suppressor, immunomodulator, and antioxidant protein, but molecular mechanism of these activities remained to be identified. Based on putative calcium-binding and myristoyl-binding domains that we identified in Fus1, we explored our hypothesis that Fus1 regulates mitochondrial calcium handling and calcium-coupled processes. ***Results:*** Fus1 loss resulted in reduced rate of mitochondrial calcium uptake in calcium-loaded epithelial cells, splenocytes, and activated $CD4^+$ T cells. The reduced rate of mitochondrial calcium uptake in Fus1-deficient cells correlated with cytosolic calcium increase and dysregulation of calcium-coupled mitochondrial parameters, such as reactive oxygen species production, $\Delta\mu H^+$, mitochondrial permeability transition pore opening, and GSH content. Inhibition of calcium efflux *via* mitochondria, Na^+/Ca^{2+} exchanger significantly improved the mitochondrial calcium uptake in $Fus1^{-/-}$ cells. *Ex vivo* analysis of activated $CD4^+$ T cells showed Fus1-dependent changes in calcium-regulated processes, such as surface expression of CD4 and PD1/PD-L1, proliferation, and Th polarization. $Fus1^{-/-}$ T cells showed increased basal expression of calcium-dependent NF-κB and NFAT targets but were unable to fully activate these pathways after stimulation. ***Innovation:*** Our results establish Fus1 as one of the few identified regulators of mitochondrial calcium handling. Our data support the idea that alterations in mitochondrial calcium dynamics could lead to the disruption of metabolic coupling in mitochondria that, in turn, may result in multiple cellular and systemic abnormalities. ***Conclusion:*** Our findings suggest that Fus1 achieves its protective role in inflammation, autoimmunity, and cancer *via* the regulation of mitochondrial calcium and calcium-coupled parameters. *Antioxid. Redox Signal.* 20, 1533–1547.

Introduction

CALCIUM IS AN ANCIENT signal transduction element that acts as a ubiquitous second messenger in a wide range of different cells and tissues. Calcium handling (uptake and release) by mitochondria regulates basal mitochondrial activities, such as energy production, but is also critical for buffering and shaping of cytosolic calcium rises that in turn regulate a plethora of signaling pathways involved in contraction, proliferation, differentiation, secretion, metabolism, apoptosis, and gene expression (2, 47, 63). Only recently have proteins involved in mitochondrial calcium handling begun to emerge (4, 14, 40, 50, 66, 67), but full understanding of mitochondrial calcium handling is far from complete. Here, we identify that Fus1 plays a critical role in mitochondrial Ca^{2+} handling and that calcium-dependent mitochondrial and cellular functions are considerably altered in cells lacking Fus1.

[1]Department of Biochemistry and Cancer Biology, VICC, Meharry Medical College, Nashville, Tennessee.
[2]Departments of Surgery and [4]Pathology, Yale School of Medicine, New Haven, Connecticut.
[3]Yale Cancer Center, Yale School of Medicine, New Haven, Connecticut.
[5]Department of Immunobiology, and Howard Hughes Medical Institute, Yale School of Medicine, New Haven, Connecticut.

Innovation

Mitochondrial calcium handling (uptake and release) regulates not only basal mitochondrial activities such as energy production but is also critical for calcium rises that regulate contraction, proliferation, differentiation, secretion, metabolism, immune response, and gene expression. We establish Fus1 as novel regulator of calcium handling and metabolic coupling of mitochondrial parameters during T-cell activation. We found that Fus1 plays a major role in the regulation of multiple calcium-dependent T-cell effector functions and proper activation of NF-κB- and NFAT-dependent pathways that rely on intracellular Ca^{2+} oscillations and reactive oxygen species. Our findings suggest that Fus1 achieves its protective role in inflammation, autoimmunity, and cancers *via* the regulation of mitochondrial calcium and calcium-coupled parameters.

The 110 a.a. FUS1/TUSC2 protein is a tumor suppressor that we recently associated with mitochondrial activities. The *Fus1* gene resides in the 3p21.3 chromosomal region that is frequently deleted in cancers (31, 51). Moreover, *Fus1* expression is epigenetically suppressed by reactive oxygen species (ROS) in normal human and mouse cells (31, 62), suggesting that patients with chronically increased ROS (smoking) will have low *Fus1* expression in exposed tissues and organs. Loss of Fus1 in mice results in an autoimmune-like syndrome with chronic inflammation and spontaneous formation of both vascular tumors and lymphomas (30). Following exposure to asbestos, Fus1 knockout (KO) mice have an altered acute inflammatory response, including unbalanced production of key pro- and anti-inflammatory cytokines (62). At the cellular level, Fus1 regulates mitochondrial homeostasis in both tumor and immune cells (62), but the molecular activities of Fus1 responsible for its systemic effects remained unclear. Here, based on protein context analysis, we suggested that Fus1 belongs to the Ca^{2+}-myristoyl switch protein family and is involved in the regulation of Ca^{2+} handling. We report that Fus1 alters mitochondrial Ca^{2+} uptake and other parameters ($\Delta\mu H^+$ alteration, ROS and nitric oxide [NO] production, mitochondrial permeability transition pore [mPTP] opening, and GSH redox status) in normal epithelial and immune cells and explore possible mechanisms of the Fus1 activity. We show that Fus1 is required for coordinated and balanced mitochondrial changes during $CD4^+$ T-cell activation, as well as for T-cell effector Ca^{2+}-dependent activities. At the molecular level, we demonstrate that Fus1 loss in $CD4^+$ T cells results in increased expression of Ca^{2+}-regulated proteins at a steady state and underactivation of the NF-κB- and NFAT-dependent pathways after CD3/CD28 activation identifying Fus1 as a novel regulator of mitochondrial Ca^{2+} uptake and immune activities that rely on Ca^{2+} signaling.

Results

FUS1/TUSC2 is a potential Ca^{2+}-binding protein

To gain insight into biological and molecular activities of Fus1, pairwise sequence alignment and analysis of Fus1 similarity with other proteins was performed using LALIGN at http://fasta.bioch.virginia.edu/fasta_www2/fasta_www.cgi?rm=lalign. A Fus1 protein fragment (pos. 54–65 a.a) was found to be highly homologous to the Ca^{2+}-binding domains (EF-hands) of the canonical EF-hand protein, calmodulin, as well as to EF-hand domains of the mitochondrial proteins MICU1 (50) and LETM1 (32) (Fig. 1A).

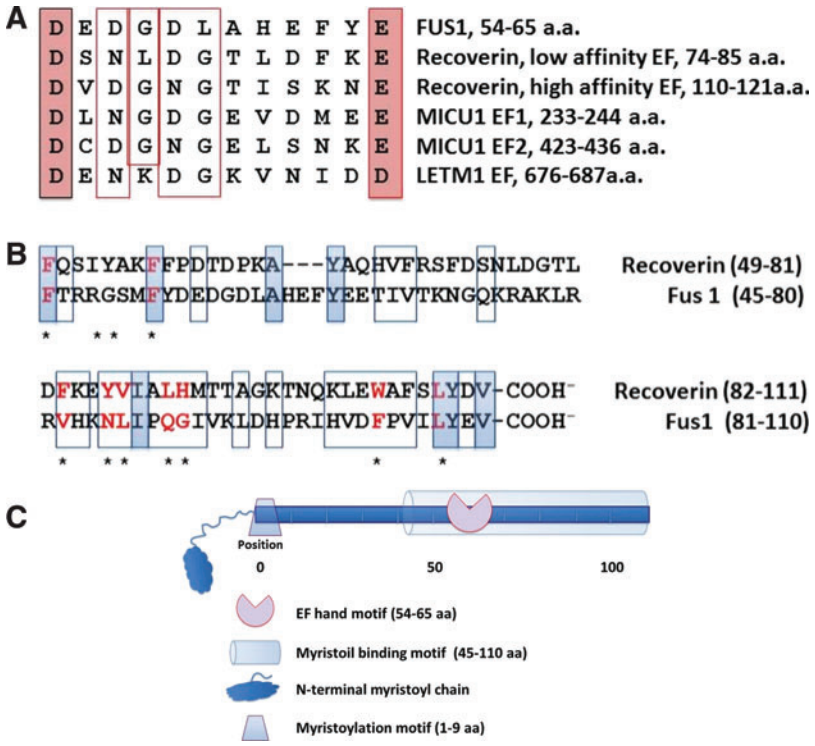

FIG. 1. Schematic diagram of the Fus1 protein domain structure deduced from multiple alignment shows key elements of the myristoyl-switch protein family. (A) The amino-terminal sequence of Fus1 fits consensus for EF-hand domains in recoverin and mitochondrial Ca^{2+}-binding proteins. **(B)** Alignment of the Fus1 N-terminal fragment (pos. 45-110 a.a) and a myristoyl-binding domain of recoverin. Conserved positions are shown in *shaded rectangles*; chemically similar amino acids are indicated with *open rectangles*. Key amino acids that compose the myristoyl-binding hydrophobic pocket of recoverin are marked with *asterisks* and presented in red if they are identical or chemically similar to the corresponding residues in the Fus1 protein. **(C)** Schematic representation of the Fus1 protein domain structure. To see this illustration in color, the reader is referred to the web version of this article at www.liebertpub.com/ars

Identification of a putative Ca^{2+}-binding domain (this study) combined with a previously described N-myristoylation site crucial for the Fus1 activity (61) prompted the comparison of Fus1 structure to recoverin and other members of the Ca^{2+}/myristoyl switch protein family (1, 57). A long N-terminal fragment of FUS1 (pos. 45–110 a.a.) has 53% homology to the myristoil-binding domain of recoverin (57) (Fig. 1C). Importantly, 9 of 11 key amino acids (82%) that form myristoyl-binding hydrophobic pocket of recoverin are identical or chemically similar in the Fus1 protein (Fig. 1C), suggesting that the 45–110 a.a. fragment of Fus1 may function as a myristoyl-binding site. Thus, our *in silico* analysis suggests that Fus1 may act as a Ca^{2+}/myristoyl switch protein and its activity may be linked to mitochondrial Ca^{2+} handling. This hypothesis is supported by our data on Fus1 involvement in the regulation of mitochondrial membrane potential (MMP) and ROS production (62), two processes that rely on mitochondrial Ca^{2+} homeostasis (7, 8).

Fus1 modulates Ca^{2+} uptake by mitochondria through Na^+/Ca^{2+} exchanger

To establish the role of Fus1 in Ca^{2+} handling, mitochondrial calcium (mitoCa^{2+}) accumulation was estimated in spontaneously immortalized Fus1 wild-type (WT) and Fus1 KO epithelial cells using fluorescence intensity changes of the mitoCa^{2+} sensor Rhod-2. Compared to WT cells, KO cells had significantly elevated basal mitoCa^{2+} levels but accumulated significantly less mitoCa^{2+} in response to the pretreatment with Ca^{2+} plus ionomycin (IO), a Ca^{2+} ionophore (Fig. 2A). To confirm these results, we measured Ca^{2+} uptake by energized mitochondria after a mild permeabilization of cells with digitonin that leaves intracellular ER and mitochondria membranes intact. Mitochondria of permeabilized WT cells took up added Ca^{2+} at an average rate of 580 ± 91.2 RFU/min, whereas buffering by permeabilized Fus1 KO cells was approximately ninefold less at a rate of

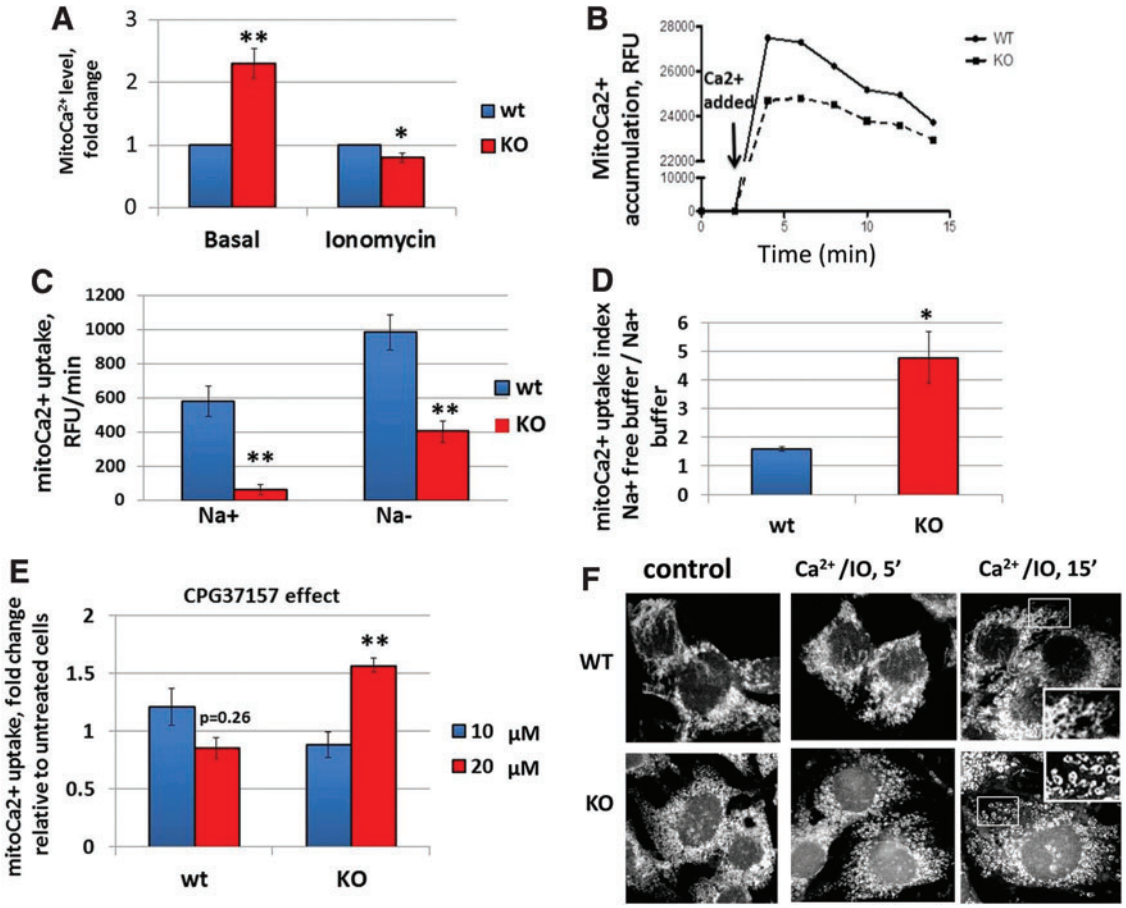

FIG. 2. Fus1 modulates mitochondrial Ca^{2+} uptake through Na^+/Ca^{2+} exchanger and maintains basal and Ca^{2+}-induced mitochondrial fusion in normal epithelial cells. **(A)** Relative basal and Ca^{2+}/IO-induced levels of mitoCa^{2+} in Fus1 KO and WT immortalized epithelial cells. **(B)** Representative curve of mitochondrial Ca^{2+} dynamics in digitonin-permeabilized Fus1 KO and WT epithelial cells using Calcium Green-5N. *Arrow* denotes the addition of a pulse of $CaCl_2$ (100 μM). **(C)** The absolute rates of mitoCa^{2+} uptake in digitonin-permeabilized Fus1 KO and Fus1 WT epithelial cells incubated in Na^+-containing (Na^+) and Na^+-free buffer ($Na-$). **(D)** MitoCa^{2+} uptake indices (Ca^{2+} uptake in Na-free/Ca^{2+} uptake in Na^+ buffer) in Fus1 KO and WT epithelial cells. **(E)** Effect of CGP37157 on mitochondrial Ca^{2+} uptake in digitonin-permeabilized epithelial cells. **(F)** Morphology of the mitochondria in immortalized kidney Fus1 KO and WT epithelial cells. Cells were preincubated with PBS/Ca^{2+} (control) and PBS/Ca^{2+}/IO (Ca^{2+}-loading conditions) for 5 and 15 min after staining with a mitochondria-specific dye Mitotracker Red. Detailed images of fusion (WT, upper panel) and fission (KO, lower panel) are shown in the insets. Data represent mean ± SE; *p*-values are designated as *, <0.05; **, <0.01. IO, ionomycin; KO, knockout. To see this illustration in color, the reader is referred to the web version of this article at www.liebertpub.com/ars

64 ± 29 RFU/min resulting in lower levels of accumulated Ca^{2+} (Fig. 2B).

mitoCa^{2+} accumulation is a dynamic process balanced by the uptake and release of Ca^{2+} ions. The major route of calcium efflux from mitochondria involves exchange of Na^+ ions for Ca^{2+} ions through the mitochondrial Na^+/Ca^{2+} exchanger (mNCX) (48) suggesting that the slower rate of mitoCa^{2+} accumulation by Fus1 KO cells may be associated with elevated activity of mNCX. To block mNCX, permeabilized epithelial cells were preincubated in Na^+-free buffer and then loaded with Ca^{2+}. The rate of mitoCa^{2+} accumulation in Na^+-depleted media was increased both in WT (984 ± 105.2 RFU/min) and KO cells (402 ± 62.3 RFU/min) (Fig. 2C); however, in Fus1 KO cells, Ca^{2+} uptake index (rate in Na-free buffer/rate in Na^+ buffer) was threefold higher (Fig. 2D). To confirm Fus1-dependent regulation of mitoCa^{2+} transport *via* mNCX, cells were treated with the specific mNCX inhibitor, benzothiazepine CGP37157. In WT cells, a maximal effect of mNCX inhibition was observed at 10 μM of CGP37157 reflected in 20% increase in mitoCa^{2+} uptake compared to untreated cells. In Fus1 KO cells, treatment with 20 μM CGP37157 resulted in the maximal mNCX inhibition that led to 60% increase in mitoCa^{2+} uptake (Fig. 2E). These data suggest that Fus1 is required for mitoCa^{2+} accumulation that may be modulated *via* mitochondrial Na^+/Ca^{2+}exchanger.

Prevalence of mitochondrial fission in Fus1 KO cells

Mitochondrial fission and fusion play critical roles in maintaining functional mitochondria when cells experience metabolic or environmental stresses. The balance of these processes is important for the maintenance of mitochondrial DNA, mitochondrial respiration, ROS and ATP production, Ca^{2+} uptake, cell proliferation, and autophagy (22, 49). We evaluated changes in mitochondrial morphology of Fus1 WT and Fus1 KO epithelial cells induced by Ca^{2+}/IO treatment. As shown in Figure 2F, at a basal state, WT mitochondria formed filamentous/granular network while Fus1 KO mitochondria are represented by granular structures. Ca^{2+} overload induced mostly fusion in mitochondrial networks of WT cells with only minor signs of fission, whereas Fus1 KO cells exhibited profound fission with fragmentation into ring-shaped mitochondria (Fig. 2F). Thus, mitochondrial fission prevailed in Fus1 KO cells at a basal level and upon Ca^{2+} overload.

Fus1 maintains mitochondrial homeostasis in immune cells

Calcium as a second messenger is involved in metabolic coupling. Ca^{2+} ions stimulate several dehydrogenases of the Krebs cycle and thus elevate MMP ($\Delta\mu H^+$) (24). In turn, elevated $\Delta\mu H^+$ induces ROS production (41). At the same time, during injury, alterations in $\Delta\mu H^+$, mitoCa^{2+}, and mitoROS may promote opening of the mPTP, release of cytochrome *c*, and cell death (26). We performed a detailed comparative analysis of major Ca^{2+}-dependent parameters, such as mitoCa^{2+}, cytoCa^{2+} (measured with fluoro-3 acetoxymethyl ester [Fluo-3/AM]), $\Delta\mu H^+$ (measured with JC-1), mitoROS (measured with MitoSOX), and mPTP permeability (calcein) in Fus1 KO and WT splenocytes. We chose immune cells for this analysis since Fus1 plays a complex and not yet fully understood role in the immune system (30, 62). Relative to WT levels, the basal mitoCa^{2+} level was significantly higher in Fus1 KO cells, whereas the cytoCa^{2+} level was lower (Fig. 3A) suggesting that Fus1 negatively regulates steady-state Ca^{2+} handling by mitochondria. Accordingly, basal levels of Ca^{2+}-dependent parameters $\Delta\mu H^+$, mitoROS, and mPTP permeability were higher in Fus1 KO cells (Fig. 3A). Overall, these results and our earlier findings (62) characterize Fus1 as a novel factor controlling steady-state mitochondrial Ca^{2+} homeostasis.

Fus1 is required for a measured response to Ca^{2+} agonist IO in splenocytes

Since Ca^{2+} transport plays an important role in the lymphocyte fate (25, 58, 60), changes in the levels of mitoCa^{2+}, cytoCa^{2+}, $\Delta\mu H^+$, nonprotein thiols, including glutathione (referred to thereafter as GSH, measured with Green CMFDA [5-chloromethylfluorescein diacetate]), NO (measured with DAF-FM), and mPTP permeability, were determined in WT and Fus1 KO splenocytes after IO treatment. Combination of IO and phorbol ester (*e.g.,* PMA) allows to bypass signals from T-cell receptors resulting in Ca^{2+} elevation, T-cell activation, and production of IL-2, IL-4, IFN-γ, *etc.* (25).

Splenocytes were gradually loaded with increased concentrations of Ca^{2+} or IO and rates of intracellular Ca^{2+} accumulation measured in WT and Fus1 KO splenocytes. Experimental conditions included gradually increased Ca^{2+} concentration (10 μM–1 mM) at a constant IO (200 nM) and gradually increased IO concentration (400–1600 nM) at a constant Ca^{2+} (1 mM).

Fold-change in Ca^{2+} accumulation and other parameters was calculated as a ratio of fluorescent dye intensities in Ca^{2+}/IO-treated cells (F) to control cells treated with Ca^{2+} only (F_o). As shown in Figure 3B, alterations in cytoCa^{2+} level at IO presence resulted in changes of other mitochondrial parameters, such as mitoCa^{2+}, $\Delta\mu H^+$, ROS, mPTP permeability, GSH, and NO.

At 1 mM extracellular Ca^{2+} concentration, the curves for cytoCa^{2+}, mitoCa^{2+}, and $\Delta\mu H^+$ (Fig. 3B) reached a plateau indicating that the system reached a saturation point that could not be changed even by increasing of IO concentration (up to 1600 nM).

Analysis of transduction of cytoCa^{2+} into mitoCa^{2+} showed that, in general, the accumulation of cytoCa^{2+} results in exponential increase in mitoCa^{2+}, which was consistent with similar studies on Ca^{2+} accumulation (13). In WT cells, any small alterations of cytoCa^{2+} level resulted in significant changes in Ca^{2+} uptake by mitochondria reflected in a steep curve of mitoCa^{2+} accumulation (Fig. 3C). Fus1 loss led to a blunted Ca^{2+} response and a rightward shift of the mitoCa^{2+} accumulation curve suggesting suppression of Ca^{2+} uptake and/or elevated Ca^{2+} efflux by Fus1 KO mitochondria (Fig. 3C). Observed differences were calculated as EC_{50} values that were 60% higher for Fus1 KO cells compared to WT cells (Fig. 3C, bar graph). Calcium has a dual effect on $\Delta\mu H^+$: matrix Ca^{2+} elevates $\Delta\mu H^+$ due to its stimulatory effect on tricarbonic acid cycle and concomitant increase in proton pumping, whereas excess of Ca^{2+} uptake leads to $\Delta\mu H^+$ depolarization because of energy dissipation (13). Figure 3C depicts logistic curves describing the transmission of mitoCa^{2+} level into $\Delta\mu H^+$ changes. Fus1 loss results in a

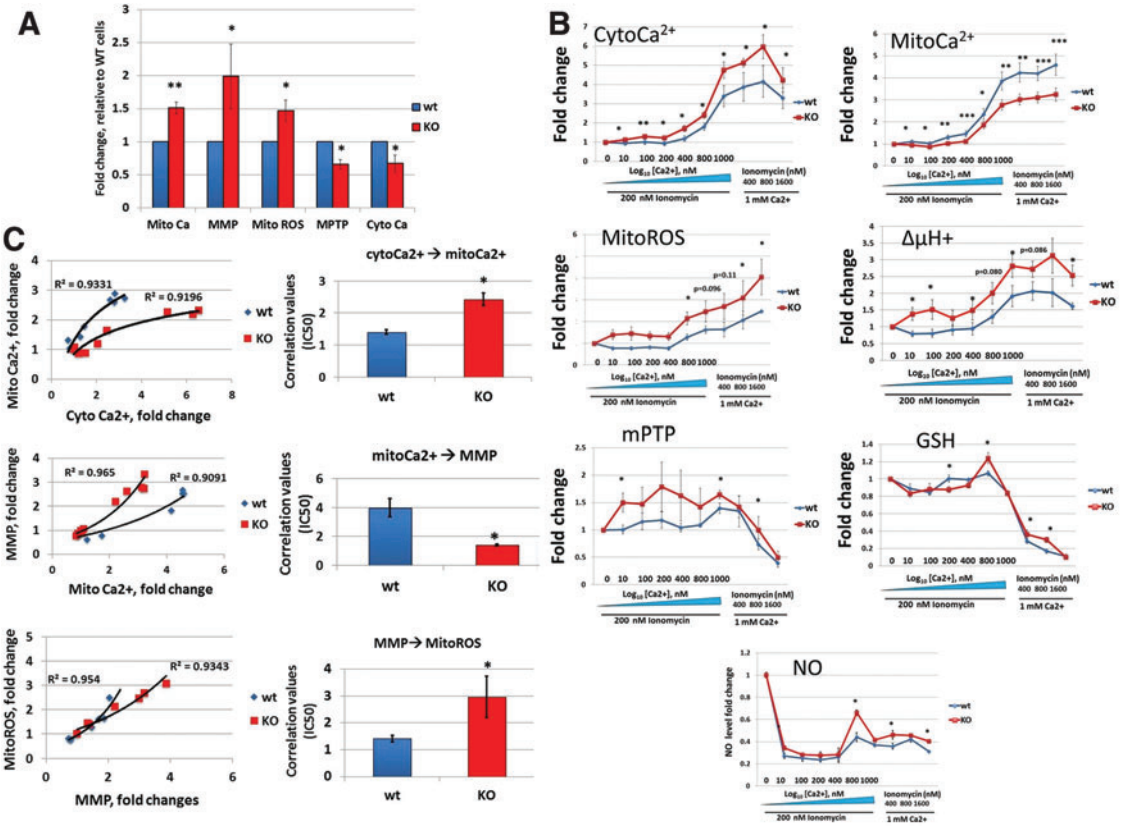

FIG. 3. Fus1 is required for the maintenance of basal mitochondrial homeostasis and for mitochondrial response to Ca^{2+} overload in immune cells. (A) Fus1-dependent changes in basal mitochondrial parameters coupled with Ca^{2+} dynamics measured in splenocytes isolated from Fus1 WT and Fus1 KO mice ($n=5$). Results are expressed as fold changes relative to WT cells. **(B)** Dynamics of changes in major mitochondrial parameters upon increasing of calcium load in splenocytes of WT and Fus1 KO mice ($n=5$–6/group). Results are presented as fold changes in relative fluorescence (RF) values compared to control cells normalized to 1.0. **(C)** Analysis of the efficiency of transduction of coupled mitochondrial parameters in WT and KO splenocytes under conditions of increasing calcium load. Correlation values were calculated as IC50 and presented as mean ± SE. IC50 was calculated in accordance with general rules applied for determination in values of effectiveness of parameters transformation restored from a series of dose–response data as described elsewhere (45). Data represent mean ± SE; *p*-values are designated as *, <0.05; **, <0.01; ***, <0.001. To see this illustration in color, the reader is referred to the web version of this article at www.liebertpub.com/ars

leftward shift of $\Delta\mu H^+$ curve reflecting more effective (2.6-fold) transduction of mitoCa^{2+} level into $\Delta\mu H^+$ at all used concentrations of Ca^{2+} and IO (Fig. 3C, left panel). Considering that upon increasing of Ca^{2+} load the rate of mito-Ca^{2+} uptake in Fus1 KO cells is lower than in WT cells (Fig. 3C, bar graph), we suggest that the decreased mitoCa^{2+} uptake may prevent depolarizing effect of Ca^{2+} on $\Delta\mu H^+$ in Fus1 KO cells.

Mitochondria are a dominant cellular source of ROS under normal conditions. ROS production is determined by the $\Delta\mu H^+$ magnitude and is increased nonlinearly with $\Delta\mu H^+$ elevation (6). Indeed, production of ROS in WT and Fus1 KO splenocytes was increased upon treatment with Ca^{2+}/IO in accordance with $\Delta\mu H^+$ changes (Fig. 3C). However, in Fus1 KO cells, transformation of $\Delta\mu H^+$ into ROS production was less efficient despite higher efficiency of transduction of mitoCa^{2+} into $\Delta\mu H^+$ (Fig. 3C).

mPTP opening triggered by the elevated Ca^{2+} in the mitochondrial matrix increases mitochondrial membrane permeability and causes $\Delta\mu H^+$ de-polarization, decrease in ATP, and increase in ROS productions. The fate of the cell after an insult depends on the extent of mPTP opening. If mPTP opens slightly, the cell may recover, whereas if it opens further, the cell may undergo apoptosis or necrosis dependent on the degree of opening (26). We showed that Ca^{2+}-induced mPTP permeability was lower in Fus1 KO cells compared to Fus1 WT cells (Fig. 3C), suggesting that the Fus1 activity is involved in proper and timely mPTP opening under conditions resulting in Ca^{2+} overload.

GSH plays a central role in the removal of hydrogen peroxide produced by the respiratory chain and have the highest impact on the mitochondria redox status (68). GSH levels control mPTP permeability, $\Delta\mu H^+$, NO production, and a release of calcium to the cytosol (3, 68). In our Ca^{2+}-loading experiments, GSH changes were reflected in a three-phase curve: (i) moderate drop at low Ca^{2+} concentrations (0–400 μM); (ii) moderate elevation induced by higher Ca^{2+} concentrations (800 μM), and (iii) dramatic drop at the highest Ca^{2+} concentration (1 mM) (Fig. 3B). Despite the fact that Ca^{2+}-induced increase in the GSH level occurs earlier in Fus1 WT cells (Phase 1), the overall GSH levels at Ca^{2+}-overloaded conditions (Phases 2 and 3) were higher in Fus1 KO cells (Fig. 3B).

NO is a signaling molecule produced in a Ca^{2+}-dependent manner by NO synthases (NOS), including mitochondrial NOS (15). Elevated levels of NO inhibit mitochondrial Ca^{2+} uptake thus forming a negative feedback loop (59). We found that Ca^{2+} elevation results in changes in the NO production reflected in a three-phase curve similar to GSH alterations (Fig. 3B). Like GSH, overall synthesis of NO was elevated in Fus1 KO splenocytes (Fig. 3B).

Altogether, these data demonstrated that the Fus1 activity is required for mitoCa^{2+} uptake and for mitochondrial activities coupled with Ca^{2+} ($\Delta\mu H^+$ alteration, ROS and NO production, mPTP opening, and GSH redox status).

Fus1 is required for coordinated and balanced changes of mitochondrial parameters during CD3/CD28 activation of $CD4^+$ T lymphocytes

The signaling network that mediates the activation of T lymphocytes is tightly linked with the dynamic alterations in the levels of cytoCa^{2+}, mitoCa^{2+}, $\Delta\mu H^+$, ROS, and mPTP activity (20, 52). Given that Fus1 was required for normal mitochondrial response to Ca^{2+} and that Fus1 KO mice have immune abnormalities, the role of Fus1 in early mitochondrial changes upon T-lymphocyte activation was explored. CD3/CD28 activation of WT T cells resulted in minor deviations of cytoCa^{2+} from its basal level at 0.5, 1, 3, and 4 h of stimulation (0.98 ± 0.02, 1.08 ± 0.03, 0.96 ± 0.01 and 0.95 ± 0.03-fold changes, respectively) (Fig. 4). In contrast, a steady accumulation of cytoCa^{2+} was observed in Fus1 KO T lymphocytes at 0.5 h (1.01 ± 0.02), 1 h (1.14 ± 0.03), 3 h (1.28 ± 0.09), and 4 h (1.39 ± 0.09) after CD3/CD28 stimulation (Fig. 4). Parallel measurement of mitoCa^{2+} levels showed that mitochondria of WT T cells steadily accumulated Ca^{2+} during 4 h: 1.21 ± 0.01-fold change at 0.5 h, 1.65 ± 0.03-fold at 1 h, 2.30 ± 0.07-fold at 3 h, and 2.6 ± 0.2 at 4 h of stimulation (Fig. 4). In contrast, an initial rise of mito-Ca^{2+} (1.33 ± 0.01-fold) was observed in Fus1 KO T cells 0.5 h after stimulation, it plateaued between 1 and 3 h (1.57 ± 0.02-fold; 1.66 ± 0.08-fold) before decreasing at 4 h (1.40 ± 0.04-fold) after stimulation (Fig. 4). Thus, CD3/CD28 activation of Fus1 KO $CD4^+$ T cells led to a slower rate and shorter duration of mitoCa^{2+} accumulation. These results corroborate the results from Fus1 KO splenocytes after Ca^{2+} overload (Fig. 3C) or stimulation with IO (Fig. 3B) and suggest that Fus1 KO T cells' mitochondria are characterized by impaired Ca^{2+} uptake resulting in cytosolic accumulation of Ca^{2+}.

The $\Delta\mu H^+$ and mitoROS changes at 0.5 and 1 h of T-cell activation were similar in Fus1 WT and Fus1 KO T cells. However, stimulation of Fus1 KO T cells for 3 and 4 h resulted in significantly lower magnitude of $\Delta\mu H^+$ and mitoROS compared to WT T cells (Fig. 4).

The dynamics of activation-induced mPTP changes was drastically different between WT and Fus1 KO $CD4^+$ T cells at all analyzed time points. In WT T cells, activation resulted in a gradual closing of mPTP between 0 and 4 h (Fig. 4). In Fus1 KO T cells, after initial pronounced closing of mPTP between 30 and 60 min, mPTP converted to an open state between 2 and 4 h post-activation (Fig. 4). At 24 h post-activation, $CD4^+$ T cells of both genotypes demonstrated an open mPTP state (data not shown).

Analysis of GSH levels at 4 h post-activation, which represents a peak time point for a CD3/CD28-induced Ca^{2+} uptake, showed no GSH changes in WT T cells, but a significant GSH decrease in Fus1 KO cells (Fig. 4, bar graph). At the same time, no differences in NO production were noted between Fus1 WT and Fus1 KO T cells (Fig. 4, bar graph).

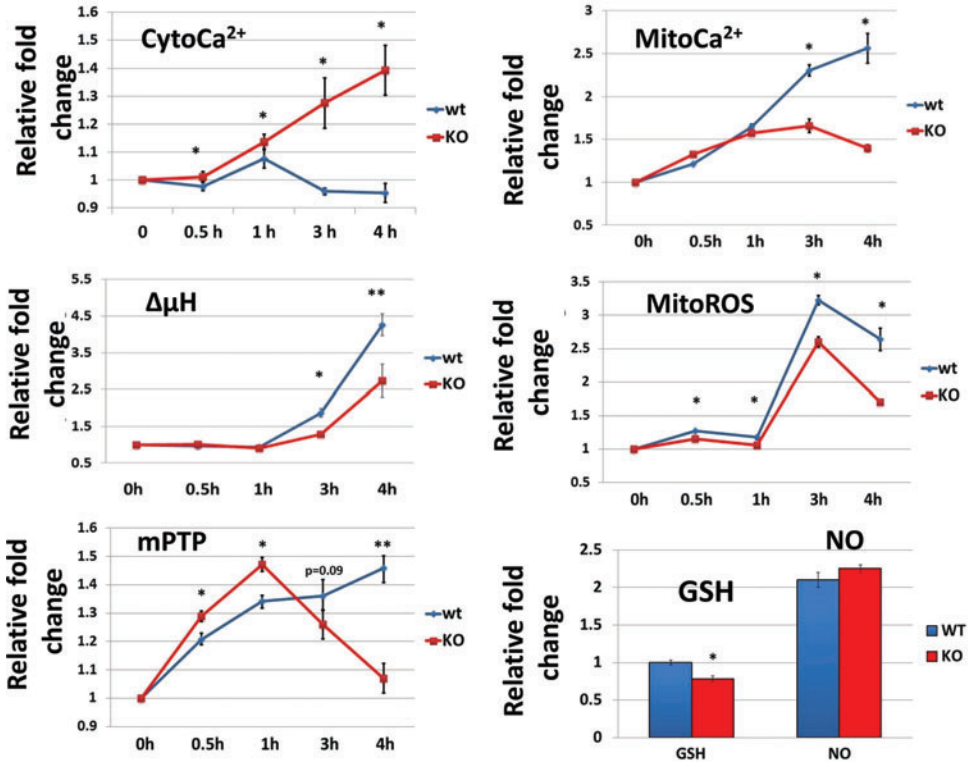

FIG. 4. Dynamic changes in Ca^{2+}-coupled mitochondrial activities induced by CD3/CD28 stimulation of $CD4^+$ T cells from Fus1 WT and Fus1 KO mice (n= 5–6/group). Results are presented as fold changes in RF values compared to control cells normalized to 1.0. Data represent mean ± SE; p-values are designated as *, <0.05; **, <0.01. To see this illustration in color, the reader is referred to the web version of this article at www.liebertpub.com/ars

Thus, alterations in GSH content may represent one of the Fus1-dependent factors affecting the activity of T cells. Taken together, our data strongly suggest that Fus1 is involved in the regulation of mitoCa^{2+} uptake capacity and alterations of Ca^{2+}-dependent mitochondrial parameters ($\Delta\mu H^+$, ROS production, mPTP opening, and GSH oxidation–reduction) during early stages of CD4$^+$ T-cell activation.

Fus1 regulates expression of surface molecules in CD4$^+$ T cells

Previously, we reported that Fus1-deficient mice develop autoimmune syndrome resembling systemic lupus erythematosus (SLE) (30). SLE is characterized by a specific pattern of cellular and molecular Ca^{2+}-dependent changes in T cells, including increased endocytic recycling of CD4 molecule (20) and increased expression of immunoregulatory molecules, such as PD-1, PD-L1, CTLA-4, and BTLA. (34). PD-1 and PD-L1 are transcriptional targets of the NF-κB complex (35, 37), whose activity is strictly dependent on the communication between mitochondria and nucleus mediated by ROS and Ca^{2+} oscillations (17, 33). Here, we compared basal surface levels of CD4 on CD4$^+$ T cells and found that Fus1 KO T cells have a slight but significantly lower basal CD4 level (Fig. 5A). CD3/CD28 activation profoundly decreased surface CD4 expression on Fus1 KO T cells after 24 h of stimulation while no changes were observed in Fus1 WT T cells at this time. Only 48 h of activation produced a similar level of CD4 decrease in both Fus1 KO and WT cells (Fig. 5A, bar graph). Thus, the dynamics of the surface CD4 expression is dependent on Fus1 activities.

Comparison of the basal level of PD-1 and its ligand PD-L1 in T cells showed no difference between genotypes (data not shown); however, upon CD3/CD28 stimulation, upregulation of PD-1 and PD-L1 was significantly attenuated in Fus1 KO T cells (Fig. 5B) suggesting that poor immunosuppressive mechanisms in Fus1 KO animals may contribute to their autoimmune phenotype (30).

Fus1 regulates CD4$^+$ T-cell effector functions

Accumulation of mitoCa^{2+} triggers T-cell processes including Th differentiation (60), proliferation (47, 63), and apoptosis (20). To determine if Fus1 regulates T-cell differentiation, CD4$^+$ T cells were stimulated with CD3/CD28 for 36 h followed by the assessment of IFNγ and IL-4, the hallmark cytokines of Th1 and Th2 cells, respectively. Absence of Fus1 significantly increased Th1 differentiation (stimulation index or IFNγ-fold increase, WT *vs.* KO: 26.2 *vs.* 45.7-fold, $p < 0.05$) (Fig. 5D). Concomitantly, the stimulation

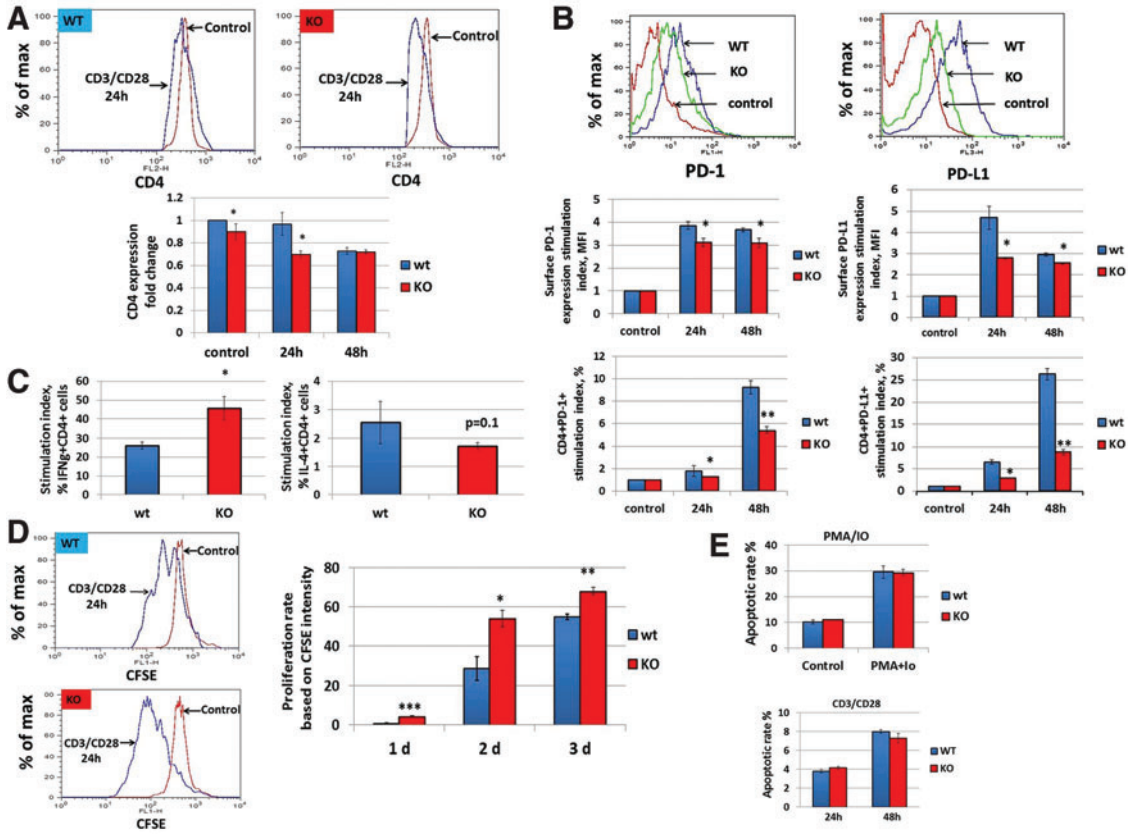

FIG. 5. Fus1 modulates Ca^{2+} mobilization-dependent processes during CD4$^+$ T- cell activation. (A, B) Effect of Fus1 loss on the dynamic changes in surface levels of CD4 and **(B)** PD-1/PD-L1 molecules during CD3/CD28 stimulation of WT and Fus1 KO CD4$^+$ T lymphocytes. **(C–E)** Fus1-dependent changes in the effector functions of activated CD4$^+$ T cells, such as Th differentiation, which was defined based on preferential expression of IFNγ (Th1 cell marker) or IL-4 (Th2 cell marker) **(C)**, proliferation **(D)**, and apoptosis **(E)**. Data represent mean ± SE; *p*-values are designated as *, <0.05; **, <0.01; ***, <0.001. To see this illustration in color, the reader is referred to the web version of this article at www.liebertpub.com/ars

index for IL-4 production was lower in Fus1 KO $CD4^+$ T cells although the difference did not reach statistical significance (WT *vs.* KO: 2.55 *vs.* 1.72, $p=0.1$) (Fig. 5D). These data suggest that Fus1 inhibits Th1 differentiation following CD3/CD28 stimulation and thus affects the Th1/Th2 cytokine axis. To assess the proliferative capacity of $CD4^+$ T cells under conditions simulating a strong antigen signal, purified T cells were labeled with CFSE and stimulated with CD3/CD28 antibodies. As shown in Figure 5D, Fus1 WT $CD4^+$ T cells had little to no proliferative response to the stimulation at day 1 with a marked increase in the proliferation rate at day 2 and robust proliferation at day 3 post-activation. In contrast, proliferation of Fus1 KO $CD4^+$ T cells was detectable at day 1 and remained higher throughout the experimental time course of stimulation (Fig. 5E). These results indicate that Fus1 suppresses proliferative capacity of $CD4^+$ T cells following short-term (1 day) and extended stimulation.

Data presented here support Fus1 as a regulator of mito-Ca^{2+} uptake, $\Delta\mu H^+$, ROS production, and mPTP permeability after IO and CD3/CD28 stimulation. In addition, Fus1 loss results in an autoimmune-like syndrome and regulated Th proliferation after stimulation. To determine if Fus1 also alters primary Th-cell apoptosis, T cells were activated with PMA/IO or CD3/CD28 and apoptosis was measured by annexin and PI staining after 9 h (9) and 24–48 h of stimulation (42), correspondingly. We were not able to detect Fus1-dependent differences in PMA + IO (Fig. 5E) or CD3/CD28-induced (Fig. 5E) apoptosis in $CD4^+$ T cells, suggesting that Fus1 activities may not be involved in T-cell apoptosis under analyzed stimulatory conditions; however, additional experiments are required to make a definitive conclusion on the role of Fus1 in T-cell apoptosis.

Fus1 KO T cells overexpress NF-κB/NFAT- and Ca^{2+}-binding proteins and Ca^{2+}-regulated genes at a steady state

To understand the mechanisms through which Fus1 deficiency affects diverse molecular pathways in T cells, transcriptional profiles of isolated WT and Fus1 KO $CD4^+$ T cells were compared. Basal expression of 222 GO-annotated genes was at least 1.5-fold higher in Fus1 KO than in WT T cells. Enrichment of canonical pathways and processes affected by Fus1 loss were identified using Genecodis and GSEA analyses (http://genecodis.cnb.csic.es/analysis and www.broadinstitute.org/gsea). Promoters of genes suppressed by Fus1 (upregulated in Fus1 KO T cells) were highly enriched in binding sites for Ca^{2+}-regulated transcription factors (TFs) NFAT, NF-κB, and C/EBP as well as for TF binding sites that synergistically cooperate with NFAT (MAF, IRF, and OCT1) (28) (Fig 6A). Activation of these TFs depends on Ca^{2+} levels and oscillations (17), consistent with a role of Fus1 as a regulator of subcellular Ca^{2+} pools. Further support of Fus1 in Ca^{2+}-dependent signaling was provided by the upregulation of a large set of Ca^{2+}-associated genes in Fus1 KO T cells (Fig. 6B). Of interest, Retnlg (resistin), a proinflammatory cytokine, which induces a rapid increase in intracellular Ca^{2+} concentration and NF-κB activation (5), was increased approximately threefold in Fus1 KO cells. Other highly expressed genes in the absence of Fus1 were the Ca^{2+} binding and EF-hand domain-containing proteins, S100a8 and S100a9, which function mainly as a S100A8/A9 heterotetramer. S100A8/A9 expression is a hallmark of inflammatory conditions, such as rheumatoid arthritis, inflammatory bowel disease, and multiple sclerosis. (54). As both proteins are also known to induce multiple endopeptidases (64), increased expression of Mmp8, Mmp9, Adam4, Adam8, and Adam19 observed in $CD4^+$ Fus1 KO cells provided additional support for S100a8/S100a9 activation. Among the top 20 genes whose expression was inhibited by Fus1 was Triadin (Trdn, six probes), a protein of the Ca^{2+} release complex that modulates Ca^{2+} homeostasis (55); two members of Ca^{2+}-dependent C-type lectin family, Clec4d and Clec4n, and Lipocalin 2, a neutrophil Ca^{2+}-induced gene (36) (Fig. 6B). The complete list of Fus1 targets upregulated in Fus1 KO T cells is shown in Supplementary Table S1 (Supplementary Data are available online at www.liebertpub.com/ars). Interestingly, no significant enrichment of TF sites in the promoters of the genes downregulated in Fus1 KO cells could be found; however, there was a strong enrichment for genes encoding mitochondrial proteins involved in oxidation–reduction and in electron transport ($p=0.0006$ and $p=0.0008$, respectively), including NDUF proteins (Fig. 6C), supporting the idea of mitochondrial dysfunction in Fus1-deficient cells.

Fus1 deficiency in $CD4^+$ T cells inhibits the activation of CD3/CD28-dependent genes

Given that calcium uptake by mitochondria plays a crucial role during T-cell activation (52), effects of Fus1 loss on gene expression in stimulated $CD4^+$ T cells were examined. Comparison of stimulated to unstimulated WT T cells revealed upregulation of a number of well-characterized genes (*e.g.,* IRF4, IL2, TNFα) that served as positive internal controls of CD3/CD28-induced activation. Of the genes upregulated in stimulated WT cells, 119 genes that were increased ≥ 1.5-fold were considered to be induced by CD3/CD28 T-cell activation (Supplementary Table S2). Activation indices for these genes (activated level/basal level) were significantly higher in WT cells than in KO cells (Fig. 6D, left panel). Remarkably, 39% of genes upregulated in WT cells failed to be activated at all in Fus1 KO T cells (Fig. 6D and Supplementary Table S2). Comparison of the absolute expression levels of these genes at basal and activated states revealed that despite the higher basal expression of these genes in Fus1 KO T cells (Fig. 6D), the level of these genes after activation was generally lower in Fus1 KO cells than in WT cells. These results suggest that loss of Fus1 in T cells impairs proper upregulation of genes involved in response to activation.

Discussion

We previously reported that Fus1 links inflammatory response and mitochondrial homeostasis affecting $\Delta\mu H^+$, ROS, and cytokine production by activated T cells (62); however, the molecular function(s) of Fus1 in mitochondria remained unknown. Based on pairwise alignment and context analysis combined with a Fus1 N-terminal myristoylation site identified earlier (61), we explored the hypothesis that Fus1 is a Ca^{2+}/myristoyl switch protein. The members of this family change conformation and membrane attachment depending on Ca^{2+} level (1, 57, 69), thus helping to localize proteins to distinct signaling compartments and coordinate regulation of

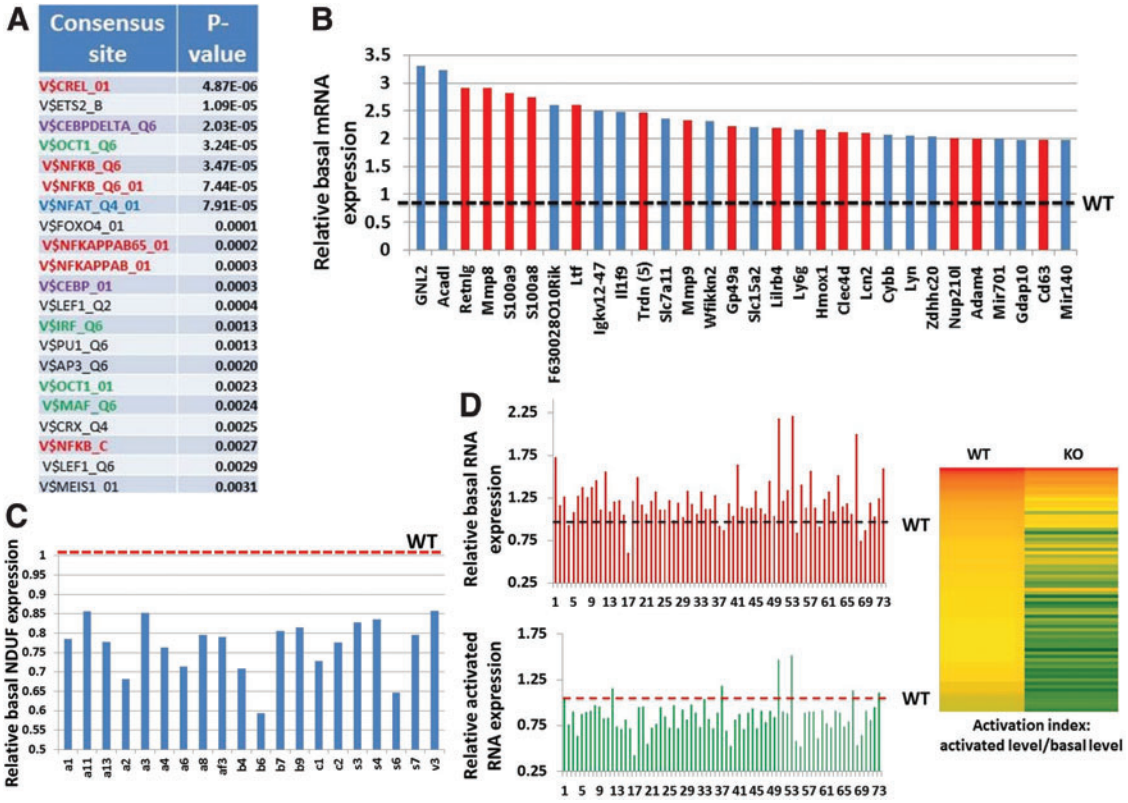

FIG. 6. Fus1-dependent expression changes observed in CD4$^+$ T cells suggest dysregulation of the Ca^{2+}-dependent NF-κB and NFAT-pathways at basal and activated conditions and mitochondrial dysfunction in Fus1 KO lymphocytes. (A) Enrichment with consensus sites for Ca^{2+}-regulated TFs (NFAT [blue], NF-κB [red], and CEBP [violet]) and TFs that synergistically cooperate with NFAT (green) in the promoters of genes upregulated at basal levels (×1.5-fold and higher) in Fus1 KO lymphocytes **(B)**. The list of top 30 genes overexpressed in unstimulated Fus1 KO T cells is enriched with genes that encode Ca^{2+}-binding and Ca^{2+}-regulated proteins (red bars). Overexpression is shown as fold change over WT expression (1.0) that is marked with *dotted black line*. **(C)** Fus1 KO T cells show global underexpression of mitochondrial proteins including a large cluster of genes that encode enzymes involved in oxidative phosphorylation (NDUF family; symbols of individual NDUF proteins are shown under X axis). Relative WT level (1.0) is marked with the *dotted red line* **(D)**. CD3/CD28-stimulated Fus1 KO T cells demonstrate global underexpression of activation response genes compared to WT cells. Bottom bar graph shows relative expression of 73 genes in Fus1 KO cells that were found activated at highest levels in WT cells. Relative WT level (WT = 1.0) is marked with the *dotted red line*. Upper bar graph shows global overexpression of the same set of genes in Fus1 KO T cells at basal conditions. Activation indices for these genes in WT and Fus1 KO T cells are presented as a color-coded diagram where highest values are shown in red and lowest values in green. For the entire list of genes, see Supplementary Table S2. To see this illustration in color, the reader is referred to the web version of this article at www.liebertpub.com/ars

Ca^{2+} signaling cascades. Our hypothetical scheme of Fus1 Ca^{2+}-dependent conformations based on its domain structure is depicted in Figure 7A.

Here, Fus1 was shown to be involved in mitochondrial Ca^{2+} handling, as well as Ca^{2+}-dependent processes and pathways (Fig. 7B). Studies presented here contribute to a better understanding of Fus1 activities with mechanistic insight. A number of conclusions have emerged from this study. First, Fus1 regulates subcellular Ca^{2+} pools *via* mitochondrial Ca^{2+} handling linked to the activity of the Na$^+$/Ca^{2+} exchanger (mNCX). Second, Fus1 controls metabolic coupling of mitochondrial parameters and efficiency of their sequential transduction *via* the regulation of mitoCa^{2+} handling. Third, Fus1 activities at basal and Ca^{2+}-overload conditions are coupled with mitochondrial dynamics (fission/fusion). Fourth, in agreement with the crucial role of calcium signals in the regulation of multiple lymphocyte functions (2, 47, 52, 63), Fus1 is required for coordinated and balanced changes in mitochondrial parameters in T cells, regulation of surface markers, T-cell proliferation, and Th1/Th2 differentiation during the activation of CD4$^+$ T cells. Fifth, in CD4$^+$ T cells, Fus1 plays a major role in the proper and timely activation of NF-κB- and NFAT-dependent pathways regulated *via* intracellular Ca^{2+} oscillations (17). Each of these points as well as our model of coupling of Ca^{2+}-dependent mitochondrial processes in Fus1 WT and Fus1 KO mitochondria are discussed below.

The maintenance of Ca^{2+} homeostasis in cells involves Ca^{2+} uptake by mitochondria regulated by the mitochondrial calcium uniporter (MCU) and Ca^{2+} efflux regulated *via* NCX. In this study, we identified Fus1 as a novel regulator of mitoCa^{2+} handling at both steady-state and Ca^{2+} overload conditions. Our data suggest that Fus1 modulates mitoCa^{2+}, at least, in part, *via* the regulation of NCX that exports one

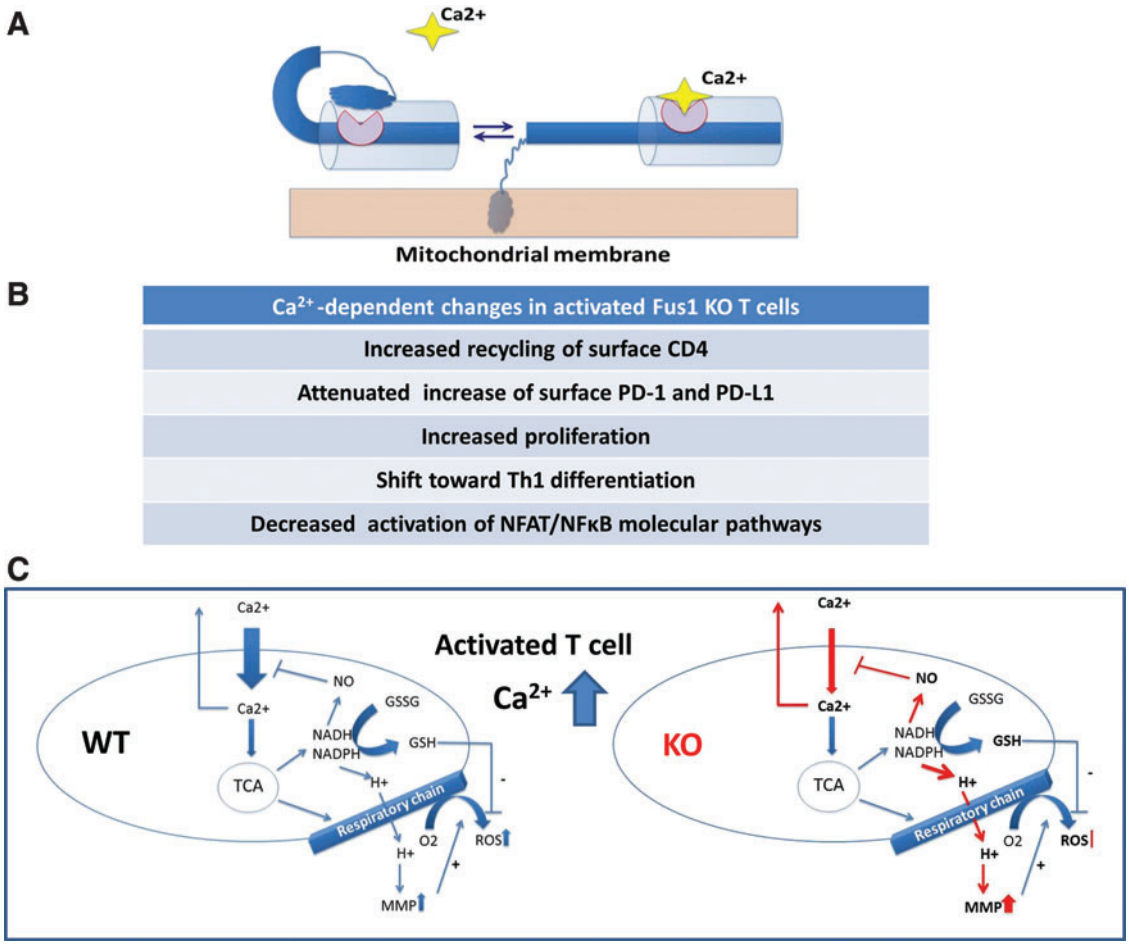

FIG. 7. Hypothetical schemes of Fus1 protein Ca^{2+}-dependent conformation changes and Ca^{2+} uptake-coupled mitochondrial events that are regulated by Fus1 activities. **(A)** Schematic diagram of proposed calcium-myristoyl switch in Fus1. The binding of one Ca^{2+} ion promotes the release of the myristoyl group from the myristoyl-binding hydrophobic pocket and anchoring of the protein in membrane structures. **(B)** The list of the Ca^{2+}-dependent processes in activated T cells affected by Fus1 loss. **(C)** Schematic representation of interactions and transitions between different mitochondrial processes and their regulation by cytosolic Ca^{2+} elevation in WT and Fus1 KO immune cells. Parameters shown in bold were tested in our study. Processes affected in Fus1 KO cells are shown with *red arrows*. For detailed description of the presented model, see Supplementary Data. To see this illustration in color, the reader is referred to the web version of this article at www.liebertpub.com/ars

Ca^{2+} ion for every three imported Na^{+} ions (11, 27, 39). Since NCX inhibition resulted in mitoCa^{2+} accumulation in Fus1 KO cells, NCX inhibitors could be considered therapeutics for treating diseases associated with Fus1 deficiency, such as cancer and autoimmunity (30).

Disrupted mitochondrial dynamics results in major cellular dysfunction that precipitates in various diseases (12, 16). Our data (Fig. 2F) suggest that Fus1 activity maintains mitochondrial fusion, which may stem from the Fus1 effect on mitoCa^{2+} handling. Mitochondrial fission/fusion cycles are balanced by a master regulator of mitochondrial biogenesis PGC-1α that is itself regulated *via* Ca^{2+} (65). Alternatively, the observed Fus1 effect on mitochondrial dynamics may come from the regulation of Ca^{2+}-dependent CaMK1a and calcineurin involved in the phosphorylation/dephosphorylation of DRP1, the main regulator of mitochondrial fragmentation (10). Further work is required to identify the important details of Fus1 involvement in this process.

Ca^{2+} influx is crucial for T-cell activation and differentiation (20, 21, 46). Using two models of lymphocyte activation, we showed that loss of Fus1 in immune cells consistently resulted in reduced mitoCa^{2+} uptake and coordinate increase of Ca^{2+} in the cytosol (Figs. 3B, C and 4A, B). Changes in subcellular Ca^{2+} pools in Fus1 KO cells were accompanied by altered dynamics of mitochondrial parameters ($\Delta\mu H^{+}$, mitoROS, mPTP permeability, NO synthesis, and GSH level), dependent on the nature of stimuli and/or duration of stimulation (Figs. 3D–H and 4C–G). These observations suggest that Fus1 is involved in fine-tuning of mitochondrial activities during T-cell activation.

Analysis of the efficiency of transduction of coupled mitochondrial parameters is a yet another way to assess the nature of Fus1-dependent pathological mitochondrial changes in immune cells. Thus, transduction of MMP into ROS in Fus1 KO cells was less efficient despite higher efficiency of transduction of mitoCa^{2+} into MMP in these cells (Fig. 3C). We explain it by compromised antioxidative cellular

mechanisms, such as NADH, NADPH, or GSH oxidation/reduction. The use of the same source (NADH) for the generation of MMP and reduction of GSH leads to a shift in MMP if reduction equivalents are redirected toward GSH synthesis (3). At the same time, reduction in mitoCa^{2+} uptake would decrease Ca^{2+}-dependent ROS generation, shift GSH oxidation, and maintain MMP elevation. Indeed, we showed that reduced mitoCa^{2+} uptake in Ca^{2+}/IO-treated Fus1 KO cells correlated with higher levels of GSH synthesis (Fig. 3C). Unbalanced Ca^{2+}-dependent ROS production and GSH synthesis is the most likely reason why transformation of MMP→ROS in Fus1 KO splenocytes is distorted. The hypothetical scheme of Fus1-dependent changes in coupled mitochondrial parameters is shown in Figure 7C.

In this study, we demonstrate that Ca^{2+}-dependent processes are also altered in Fus1 KO T cells. We found that Fus1 KO $CD4^+$ T cells have (i) a reduced basal level of the surface CD4 expression and (ii) accelerated decrease of CD4 expression following CD3/CD28 activation (Fig. 5A) that is known to be dependent on protein kinase C and NF-κB activities (53). We previously reported that Fus1 KO mice develop autoimmune syndrome resembling SLE (30). SLE is characterized by a specific pattern of changes in T cells including increased endocytic recycling of CD4 molecules through the NO→mTOR axis (20). We found earlier that $CD3^+CD4^-CD8^-$ (double negative) T cells selectively accumulated in inflammatory milieu of Fus1 KO mice are concomitant with the decrease in $CD4^+$ cell number (62). Combined, these data suggest that Fus1 is required for the maintenance of CD4 levels on unstimulated T cells, thus attenuating CD4 loss from the cell surface upon T-cell stimulation.

The PD-1/PD-L1 regulatory axis plays a central role in the suppression of autoimmune response (34). Both PD-1 and PD-L1 are transcriptional targets of NF-κB (35, 37), whose activity is strictly dependent on mitochondria-mediated ROS production (29) and Ca^{2+} oscillations (17). We showed here that Fus1 loss attenuates the upregulation of these molecules in activated T cells (Fig. 5B, C). Since PD-1 and PD-L1 are major players in the autoimmune defense, we speculate that their altered expression may precipitate the autoimmune phenotype of Fus1 KO mice (30).

It is now commonly accepted that mitochondria regulate cell cycle progression and proliferation of lymphocytes and other cell types *via* ROS production, Ca^{2+} uptake, and changes in Ca^{2+}-dependent parameters (*i.e.,* MMP de- or hyperpolarization) (47, 63). Our data linking Fus1 with intracellular Ca^{2+} regulation led us to determine if Fus1 was required for proper regulation of T cells proliferation. Indeed, Fus1 loss robustly stimulated proliferation of $CD4^+$ T cells upon activation (Fig. 5E), thus establishing dependence of one of the crucial T-cell effector functions on the Fus1 activity.

One of our most intriguing observations is a significant CD3/CD28-induced Th1 shift in Fus1 KO $CD4^+$ T cells (Fig. 5C). The relative proportion of generated Th1 versus Th2 cells plays a critical role in determining the outcome of the host immune response to an infection. Identification of the various factors involved in regulating this balance remains an active area of investigation (56). There is currently only limited data linking mitochondrial activity and cell polarization. The mitochondrial PRELI protein inhibits Th2 differentiation (56), and lower MCU activity is linked to a lower activation of Th2 cells compared to Th1 cells upon identical stimulation (60). Although these data support a role for mitochondria in Th-cell polarization, important details of this regulation have been elusive. Data presented here are consistent with augmented Th1 differentiation in the absence of Fus1 resulting from impaired mitoCa^{2+} uptake during early activation steps. Murine Th1 and Th2 lymphocytes differ in the dynamics of Ca^{2+} response since Th2 cells have more efficient mechanisms of cytoCa^{2+} clearance (18). We showed that cytoCa^{2+} level was higher in Fus1 KO $CD4^+$ T cells correlating with the slower mitoCa^{2+} uptake during first 4 h of activation (Fig. 4). Further experiments will be needed to determine if reduced clearance of cytoCa^{2+} in the absence of Fus1 stimulates Th1 differentiation at the expense of Th2.

To better understand how decreased Fus1 expression globally alters a variety of immune responses, we have explored molecular pathways dependent on Fus1. It was shown that mitoCa^{2+} uptake and release regulate the frequency of spontaneous and induced cytoCa^{2+} oscillations, which, in turn, determine the transcriptional activity of NF-κB and NFAT, two main TFs that regulate T-cell activation (17). Since NF-κB is a redox-sensitive TF (29) and ROS production is regulated by mitoCa^{2+} uptake (19), changes in mito-Ca^{2+} shift the redox balance, which will further alter NF-κB transcriptional activity. Indeed, comparison of expression profiles of Fus1 WT and Fus1 KO $CD4^+$ T cells revealed enrichment with consensus sites for binding of NF-κB, NFAT, and other calcium-regulated TFs in the promoters of genes upregulated in Fus1 KO cells at the basal level. Also, higher basal expression of Ca^{2+}-binding and Ca^{2+}-regulated proteins in Fus1 KO $CD4^+$ T cells compared to WT cells (Supplementary Table S1) is consistent with higher cytoCa^{2+} levels in Fus1 KO T cells. Remarkably, stimulated Fus1 KO $CD4^+$ T cells showed compromised activation of the NF-κB and NFAT pathways in agreement with the slower dynamics and lower amplitudes of CD3/CD28-induced mitochondrial changes (ROS, MMP, and mPTP) that we observed in these cells (Fig. 4C–E). These changes may have resulted in insufficient and (or) distorted activation of the NF-κB and NFAT proteins and aberrant expression of their targets.

Thus, correction of mitoCa^{2+} uptake in Fus1-deficient tissues may significantly improve a variety of biological Ca^{2+}-dependent processes. These data create a basis for designing therapeutic approaches for the treatment of Fus1-deficiency-based diseases, such as autoimmunity, cancer, and inflammation.

Materials and Methods

Flow cytometric analysis of cytoCa^{2+}, mitoCa^{2+}, MMP, mitoROS, and mPTP

Cytoplasmic calcium levels were measured by loading the cells with 1 μ*M* Fluo-3/AM (excitation, 506 nm; emission, 526 nm; recorded in FL-1; Molecular Probes). Mitochondrial calcium level was estimated by loading the cells with 4 μ*M* Rhod2/AM, which is compartmentalized into the mitochondria (46). Production of mitochondrial ROS (superoxide anion) was assessed fluorometrically using oxidation-sensitive fluorescent probes MitoSOX (Molecular Probes) as described elsewhere (43). $\Delta\psi m$ was quantitated using a potential-dependent J-aggregate-forming lipophilic cation

JC-1, 5,5′,6,6′-tetrachloro-1,1′,3,3′-tetraethylbenzimidazolocarbocyanine iodide (Molecular Probes). JC-1 selectively incorporates into mitochondria, where it forms monomers (fluorescence in green, 527 nm) or aggregates, at high transmembrane potentials (fluorescence in red, 590 nm) (46). Cells were incubated with 0.5 μM JC-1 for 15–45 min at 37°C before flow cytometry. Co-treatment with a protonophore, 5 μM carbonyl cyanide m-chlorophenylhydrazone (Molecular Probes), for 15 min at 37°C resulted in decreased JC-1 fluorescence and served as a positive control for the disruption of $\Delta\psi$m (46). mPTP permeability was monitored through a release of fluorescent calcein from mitochondria *via* mPTP. The fluorescence from cytosolic calcein was quenched by the addition of $CoCl_2$, whereas the fluorescence from the mitochondrial calcein was maintained. Production of NO was estimated with dye 4-amino-5-methylamino-2′,7′-difluorofluorescein diacetate (DAF-FM; Molecular Probes). Inside the cell, DAF-FM is deacetylated and retained in the cell. Nonfluorescent DAF-FM after reaction with NO forms fluorescent benzotriazole. For NO level estimation, cells were incubated with 1–5 μM DAF-FM for 1 h at 37°C. Excitation and emission maximum of DAF-FM are 495 and 515 nm, respectively (45). Oxidation of intracellular nonprotein thiols (primarily GSH) was measured using the Cell Tracker Green CMFDA probe, which has a chloromethyl group that, when reacting with thiols, gets converted into a fluorescent adduct. For GSH measurement, cells were incubated with 1 μM CMDFA for 30–60 min at 37°C. Excitation and emission maximum of CMDFA are 492 and 517 nm, respectively (23).

Antibodies and reagents

Conjugated mouse monoclonal antibodies, CD4-FITC, CD4-PE, IFNgamma-PE, IL-4-FITC, PD-1-FITC, and PD-L1-PE (Biolegend), were used for FACS. Mouse $CD4^+$ T-cell isolation kit II was purchased from Miltenyi Biotec. Probes for the measurement of cytosolic (Fluo-3) and mitochondrial Ca^{2+} (Rhod-2) were purchased from AnaSpec Inc. Probes for other mitochondrial parameters, such as membrane potential (JC-1), reactive oxygen species (MitoSOX), permeability transition pore assay, and mitochondrial morphology (MitoTracker Red), were all from Molecular Probes (Invitrogen). CGP37157, inhibitor of mitochondrial NCX, was obtained from Sigma. Calcium Green-5N for the measurement of Ca^{2+} uptake by mitochondria in digitonin-permeabilized cells was purchased from Molecular Probes (Invitrogen).

Cell culture

Mouse immortalized kidney epithelial cells were maintained in DMEM/10% FBS medium with 100 μg/ml Anti-Anti mixture (all from Gibco, Inc.) at 37°C and 5% CO_2.

Splenocyte isolation, $CD4^+$ T-cell purification and activation

$CD4^+$ cells were purified from the whole splenocyte fraction using $CD4^+$ isolation kit II (Miltenyi Biotec). $CD4^+$ cells were activated, unless otherwise indicated, with plate-bound α-CD3 (1.0 μg/ml) and soluble α-CD28 (1.0 μg/ml; both from Biolegend) and cultured at a density of $\sim 1 \times 10^6$ cells/ml in 24-well plates in RPMI-1640 medium supplemented with Anti-Anti mixture and 10% FBS.

Mitochondrial morphology imaging

Epithelial cells at $\sim$70%–80% confluency were treated with Ca^{2+} and Ca^{2+}/ionomysin for 15 mins and with Mitotracker Red. Cells were then washed and fixed in 3.7% formaldehyde for 15 mins in the dark, permeabilized, and mounted with DAPI-containing mounting media. Zeiss LSM 510 META Upright Confocal Microscope was used for analyzing mitochondrial morphology and making images.

Measurement of mitochondrial Ca^{2+} uptake capacity of digitonin-permeabilized cells

Extramitochondrial free Ca^{2+} was monitored in the presence of digitonin-permeabilized cells as described in (44, 50). Briefly, cells (2×10^6 cells/ml) were resuspended in KCl medium (125 mM KCl, 2 mM K_2HPO_4, 1 mM $MgCl_2$, 20 mM Hepes, pH 7.0) containing 5 mM glutamate, 5 mM malate, and 5 mM succinate as oxidable substrates and 0.5 μM Ca^{2+} green-5N. The plasma membranes were then selectively permeabilized with digitonin (0.01%wt/vol final). Fluorescence (Ex506/Em531 nm) was monitored at room temperature using a SynergyMX (BioTek) fluorescence spectrophotometer. The involvement of mNCX in the Ca^{2+} homeostasis was measured by the replacement of Na-containing buffer with Na-free buffer or by the addition of benzodiazepine CGP37157 (10–20 μM), a blocker of mNCX, to challenged cells.

Flow cytometric analysis of cytoCa^{2+}, mitoCa^{2+}, MMP, mitoROS, mPTP, NO, and GSH was performed as described in detail in Supplementary Data.

$CD4^+$ T-cell proliferation assay

Proliferation of $CD4^+$ T cells was measured by flow cytometry after a CFSE dilution assay as described elsewhere (38). Splenocytes were stained with CFSE (1 μM), stimulated with CD3/CD28 (1 μg/ml of each) or left unstimulated, harvested after 1, 2, and 3 days, stained for a surface CD4 expression with anti-mouse CD4 antibodies labeled with PerCP-Cy5.5 (Biolegend), and acquired on FACS Calibur flow cytometer (Beckman Coulter).

Intracellular cytokine staining

Cytokine staining and analysis was performed as described elsewhere (56). The antibodies used were anti-mouse IFNγ-FITC (1/100 μl permeabilization buffer) and α-IL4-PE (1/100 μl permeabilization buffer) (Biolegend).

Apoptosis T-cell assays

Apoptosis was monitored by flow cytometry after concurrent staining with FITC-conjugated Annexin V (Annexin V-FITC; R&D Systems) (FL-1) and 7-AAD (FL-3) as described elsewhere (46). Apoptosis rates were expressed as a shift in Annexin V binding in PI-negative cells.

$CD4^+$ T cells RNA isolation and microarray analysis

RNA from unstimulated and stimulated for 12 h with CD3/CD28 antibodies $CD4^+$ T cells collected from five animals

per group was isolated with the RNAeasy mini RNA isolation kit (Qiagen), mixed together to obtain sufficient for hybridization RNA amount, and subjected to differential expression analysis using gene 1.0 microarray platform, which was performed in the Genomic Core Facility at the Vanderbilt University.

Statistical analysis

Results are presented as mean ± SE. Comparisons between the two groups were performed using the Student's *t*-test. When analyzing statistical differences between the KO and WT mice, $p < 0.05$ was considered significant.

Acknowledgments

I wish to thank Dr. N. Issaeva for help with confocal microscopy analysis. I apologize to those colleagues whose work I could not cite owing to space limitations. This work was supported by grant 1R21ES017496-01A1 to A.V.I. and 1 SC1 CA182843-01A1 to A.S., both from the National Institutes of Health, USA.

Author Disclosure Statement

No competing financial interests exist.

References

1. Ames JB, Ishima R, Tanaka T, Gordon JI, Stryer L, and Ikura M. Molecular mechanics of calcium-myristoyl switches. *Nature* 389: 198–202, 1997.
2. Antico Arciuch VG, Elguero ME, Poderoso JJ, and Carreras MC. Mitochondrial regulation of cell cycle and proliferation. *Antioxid Redox Signal* 16: 1150–1180, 2012.
3. Aon MA, Cortassa S, Maack C, and O'Rourke B. Sequential opening of mitochondrial ion channels as a function of glutathione redox thiol status. *J Biol Chem* 282: 21889–21900, 2007.
4. Baughman JM, Perocchi F, Girgis HS, Plovanich M, Belcher-Timme CA, Sancak Y, Bao XR, Strittmatter L, Goldberger O, Bogorad RL, Koteliansky V, and Mootha VK. Integrative genomics identifies MCU as an essential component of the mitochondrial calcium uniporter. *Nature* 476: 341–345, 2011.
5. Bertolani C, Sancho-Bru P, Failli P, Bataller R, Aleffi S, DeFranco R, Mazzinghi B, Romagnani P, Milani S, Gines P, Colmenero J, Parola M, Gelmini S, Tarquini R, Laffi G, Pinzani M, and Marra F. Resistin as an intrahepatic cytokine: overexpression during chronic injury and induction of proinflammatory actions in hepatic stellate cells. *Am J Pathol* 169: 2042–2053, 2006.
6. Brookes PS. Mitochondrial H(+) leak and ROS generation: an odd couple. *Free Radic Biol Med* 38: 12–23, 2005.
7. Brookes PS, Yoon Y, Robotham JL, Anders MW, and Sheu SS. Calcium, ATP, and ROS: a mitochondrial love-hate triangle. *Am J Physiol Cell Physiol* 287: C817–C833, 2004.
8. Camello-Almaraz MC, Pozo MJ, Murphy MP, and Camello PJ. Mitochondrial production of oxidants is necessary for physiological calcium oscillations. *J Cell Physiol* 206: 487–494, 2006.
9. Catala-Rabasa A, Ndagire D, Sabio JM, Fedetz M, Matesanz F, and Alcina A. High ACSL5 transcript levels associate with systemic lupus erythematosus and apoptosis in Jurkat T lymphocytes and peripheral blood cells. *PLoS One* 6: e28591, 2011.
10. Cereghetti GM, Stangherlin A, Martins de Brito O, Chang CR, Blackstone C, Bernardi P, and Scorrano L. Dephosphorylation by calcineurin regulates translocation of Drp1 to mitochondria. *Proc Natl Acad Sci U S A* 105: 15803–15808, 2008.
11. Chaptal V, Besserer GM, Ottolia M, Nicoll DA, Cascio D, Philipson KD, and Abramson J. How does regulatory Ca2+ regulate the Na+-Ca2+ exchanger? *Channels (Austin)* 1: 397–399, 2007.
12. Chen H and Chan DC. Mitochondrial dynamics—fusion, fission, movement, and mitophagy—in neurodegenerative diseases. *Hum Mol Genet* 18: R169–R176, 2009.
13. Cortassa S, Aon MA, Marban E, Winslow RL, and O'Rourke B. An integrated model of cardiac mitochondrial energy metabolism and calcium dynamics. *Biophys J* 84: 2734–2755, 2003.
14. De Stefani D, Raffaello A, Teardo E, Szabo I, and Rizzuto R. A forty-kilodalton protein of the inner membrane is the mitochondrial calcium uniporter. *Nature* 476: 336–340, 2011.
15. Dedkova EN and Blatter LA. Modulation of mitochondrial Ca2+ by nitric oxide in cultured bovine vascular endothelial cells. *Am J Physiol Cell Physiol* 289: C836–C845, 2005.
16. Detmer SA and Chan DC. Functions and dysfunctions of mitochondrial dynamics. *Nat Rev Mol Cell Biol* 8: 870–879, 2007.
17. Dolmetsch RE, Lewis RS, Goodnow CC, and Healy JI. Differential activation of transcription factors induced by Ca2+ response amplitude and duration. *Nature* 386: 855–858, 1997.
18. Fanger CM, Neben AL, and Cahalan MD. Differential Ca2+ influx, KCa channel activity, and Ca2+ clearance distinguish Th1 and Th2 lymphocytes. *J Immunol* 164: 1153–1160, 2000.
19. Feissner RF, Skalska J, Gaum WE, and Sheu SS. Crosstalk signaling between mitochondrial Ca2+ and ROS. *Front Biosci (Landmark Ed)* 14: 1197–1218, 2009.
20. Fernandez D and Perl A. Metabolic control of T cell activation and death in SLE. *Autoimmun Rev* 8: 184–189, 2009.
21. Feske S. Calcium signalling in lymphocyte activation and disease. *Nat Rev Immunol* 7: 690–702, 2007.
22. Fulop L, Szanda G, Enyedi B, Varnai P, and Spat A. The effect of OPA1 on mitochondrial Ca(2)(+) signaling. *PLoS One* 6: e25199, 2011.
23. Gillis C, Haegerstrand A, Ragnarson B, and Bengtsson L. Rapid visualization of viable and nonviable endothelium on cardiovascular prosthetic surfaces by means of fluorescent dyes. *J Thorac Cardiovasc Surg* 108: 1043–1048, 1994.
24. Glancy B and Balaban RS. Role of mitochondrial Ca2+ in the regulation of cellular energetics. *Biochemistry* 51: 2959–2973, 2012.
25. Guo L, Urban JF, Zhu J, and Paul WE. Elevating calcium in Th2 cells activates multiple pathways to induce IL-4 transcription and mRNA stabilization. *J Immunol* 181: 3984–3993, 2008.
26. Halestrap AP. What is the mitochondrial permeability transition pore? *J Mol Cell Cardiol* 46: 821–831, 2009.
27. Hernandez-SanMiguel E, Vay L, Santo-Domingo J, Lobaton CD, Moreno A, Montero M, and Alvarez J. The mitochondrial Na+/Ca2+ exchanger plays a key role in the control of cytosolic Ca2+ oscillations. *Cell Calcium* 40: 53–61, 2006.

28. Hogan PG, Chen L, Nardone J, and Rao A. Transcriptional regulation by calcium, calcineurin, and NFAT. *Genes Dev* 17: 2205–2232, 2003.
29. Hughes G, Murphy MP, and Ledgerwood EC. Mitochondrial reactive oxygen species regulate the temporal activation of nuclear factor kappaB to modulate tumour necrosis factor-induced apoptosis: evidence from mitochondria-targeted antioxidants. *Biochem J* 389: 83–89, 2005.
30. Ivanova AV, Ivanov SV, Pascal V, Lumsden JM, Ward JM, Morris N, Tessarolo L, Anderson SK, and Lerman MI. Autoimmunity, spontaneous tumourigenesis, and IL-15 insufficiency in mice with a targeted disruption of the tumour suppressor gene Fus1. *J Pathol* 211: 591–601, 2007.
31. Ivanova AV, Ivanov SV, Prudkin L, Nonaka D, Liu Z, Tsao A, Wistuba I, Roth J, and Pass HI. Mechanisms of FUS1/TUSC2 deficiency in mesothelioma and its tumorigenic transcriptional effects. *Mol Cancer* 8: 91, 2009.
32. Jiang D, Zhao L, and Clapham DE. Genome-wide RNAi screen identifies Letm1 as a mitochondrial Ca2+/H+ antiporter. *Science* 326: 144–147, 2009.
33. Kaminski MM, Roth D, Sass S, Sauer SW, Krammer PH, and Gulow K. Manganese superoxide dismutase: a regulator of T cell activation-induced oxidative signaling and cell death. *Biochim Biophys Acta* 1823: 1041–1052, 2012.
34. Kim HK, Guan H, Zu G, Li H, Wu L, Feng X, Elmets C, Fu Y, and Xu H. High-level expression of B7-H1 molecules by dendritic cells suppresses the function of activated T cells and desensitizes allergen-primed animals. *J Leukoc Biol* 79: 686–695, 2006.
35. Kondo A, Yamashita T, Tamura H, Zhao W, Tsuji T, Shimizu M, Shinya E, Takahashi H, Tamada K, Chen L, Dan K, and Ogata K. Interferon-gamma and tumor necrosis factor-alpha induce an immunoinhibitory molecule, B7-H1, via nuclear factor-kappaB activation in blasts in myelodysplastic syndromes. *Blood* 116: 1124–1131, 2010.
36. Lee JH, Kye KC, Seo EY, Lee K, Lee SK, Lim JS, Seo YJ, Kim CD, and Park JK. Expression of neutrophil gelatinase-associated lipocalin in calcium-induced keratinocyte differentiation. *J Korean Med Sci* 23: 302–306, 2008.
37. Liang SC, Latchman YE, Buhlmann JE, Tomczak MF, Horwitz BH, Freeman GJ, and Sharpe AH. Regulation of PD-1, PD-L1, and PD-L2 expression during normal and autoimmune responses. *Eur J Immunol* 33: 2706–2716, 2003.
38. Lyons AB and Parish CR. Determination of lymphocyte division by flow cytometry. *J Immunol Methods* 171: 131–137, 1994.
39. Maack C, Cortassa S, Aon MA, Ganesan AN, Liu T, and O'Rourke B. Elevated cytosolic Na+ decreases mitochondrial Ca2+ uptake during excitation-contraction coupling and impairs energetic adaptation in cardiac myocytes. *Circ Res* 99: 172–182, 2006.
40. Mallilankaraman K, Cardenas C, Doonan PJ, Chandramoorthy HC, Irrinki KM, Golenar T, Csordas G, Madireddi P, Yang J, Muller M, Miller R, Kolesar JE, Molgo J, Kaufman B, Hajnoczky G, Foskett JK, and Madesh M. MCUR1 is an essential component of mitochondrial Ca(2+) uptake that regulates cellular metabolism. *Nat Cell Biol* 15: 123, 2012.
41. Marchi S, Giorgi C, Suski JM, Agnoletto C, Bononi A, Bonora M, De Marchi E, Missiroli S, Patergnani S, Poletti F, Rimessi A, Duszynski J, Wieckowski MR, and Pinton P. Mitochondria-ros crosstalk in the control of cell death and aging. *J Signal Transduct* 2012: 329635, 2012.
42. Mukherjee P, Sen PC, and Ghose AC. Lymph node cells from BALB/c mice with chronic visceral leishmaniasis exhibiting cellular anergy and apoptosis: involvement of Ser/Thr phosphatase. *Apoptosis* 11: 2013–2029, 2006.
43. Murakami T, Ockinger J, Yu J, Byles V, McColl A, Hofer AM, and Horng T. Critical role for calcium mobilization in activation of the NLRP3 inflammasome. *Proc Natl Acad Sci U S A* 109: 11282–11287, 2012.
44. Murphy AN, Bredesen DE, Cortopassi G, Wang E, and Fiskum G. Bcl-2 potentiates the maximal calcium uptake capacity of neural cell mitochondria. *Proc Natl Acad Sci U S A* 93: 9893–9898, 1996.
45. Nagy G, Barcza M, Gonchoroff N, Phillips PE, and Perl A. Nitric oxide-dependent mitochondrial biogenesis generates Ca2+ signaling profile of lupus T cells. *J Immunol* 173: 3676–3683, 2004.
46. Nagy G, Koncz A, and Perl A. T cell activation-induced mitochondrial hyperpolarization is mediated by Ca2+- and redox-dependent production of nitric oxide. *J Immunol* 171: 5188–5197, 2003.
47. Nunez L, Valero RA, Senovilla L, Sanz-Blasco S, Garcia-Sancho J, and Villalobos C. Cell proliferation depends on mitochondrial Ca2+ uptake: inhibition by salicylate. *J Physiol* 571: 57–73, 2006.
48. Palty R and Sekler I. The mitochondrial Na(+)/Ca(2+) exchanger. *Cell Calcium* 52: 9–15, 2012.
49. Parone PA, Da Cruz S, Tondera D, Mattenberger Y, James DI, Maechler P, Barja F, and Martinou JC. Preventing mitochondrial fission impairs mitochondrial function and leads to loss of mitochondrial DNA. *PLoS One* 3: e3257, 2008.
50. Perocchi F, Gohil VM, Girgis HS, Bao XR, McCombs JE, Palmer AE, and Mootha VK. MICU1 encodes a mitochondrial EF hand protein required for Ca(2+) uptake. *Nature* 467: 291–296, 2010.
51. Prudkin L, Behrens C, Liu DD, Zhou X, Ozburn NC, Bekele BN, Minna JD, Moran C, Roth JA, Ji L, and Wistuba, II. Loss and reduction of FUS1 protein expression is a frequent phenomenon in the pathogenesis of lung cancer. *Clin Cancer Res* 14: 41–47, 2008.
52. Quintana A, Pasche M, Junker C, Al-Ansary D, Rieger H, Kummerow C, Nunez L, Villalobos C, Meraner P, Becherer U, Rettig J, Niemeyer BA, and Hoth M. Calcium microdomains at the immunological synapse: how ORAI channels, mitochondria and calcium pumps generate local calcium signals for efficient T-cell activation. *EMBO J* 30: 3895–3912, 2011.
53. Raposo RA, Trudgian DC, Thomas B, van Wilgenburg B, Cowley SA, and James W. Protein kinase C and NF-kappaB-dependent CD4 downregulation in macrophages induced by T cell-derived soluble factors: consequences for HIV-1 infection. *J Immunol* 187: 748–759, 2011.
54. Roth J, Goebeler M, and Sorg C. S100A8 and S100A9 in inflammatory diseases. *Lancet* 357: 1041, 2001.
55. Shen X, Franzini-Armstrong C, Lopez JR, Jones LR, Kobayashi YM, Wang Y, Kerrick WG, Caswell AH, Potter JD, Miller T, Allen PD, and Perez CF. Triadins modulate intracellular Ca(2+) homeostasis but are not essential for excitation-contraction coupling in skeletal muscle. *J Biol Chem* 282: 37864–37874, 2007.
56. Tahvanainen J, Kallonen T, Lahteenmaki H, Heiskanen KM, Westermarck J, Rao KV, and Lahesmaa R. PRELI is a mitochondrial regulator of human primary T-helper cell apoptosis, STAT6, and Th2-cell differentiation. *Blood* 113: 1268–1277, 2009.

57. Tanaka T, Ames JB, Harvey TS, Stryer L, and Ikura M. Sequestration of the membrane-targeting myristoyl group of recoverin in the calcium-free state. *Nature* 376: 444–447, 1995.
58. Thiel M, Wolfs MJ, Bauer S, Wenning AS, Burckhart T, Schwarz EC, Scott AM, Renner C, and Hoth M. Efficiency of T-cell costimulation by CD80 and CD86 cross-linking correlates with calcium entry. *Immunology* 129: 28–40, 2010.
59. Thyagarajan B, Malli R, Schmidt K, Graier WF, and Groschner K. Nitric oxide inhibits capacitative Ca2+ entry by suppression of mitochondrial Ca2+ handling. *Br J Pharmacol* 137: 821–830, 2002.
60. Toldi G, Kaposi A, Zsembery A, Treszl A, Tulassay T, and Vasarhelyi B. Human Th1 and Th2 lymphocytes are distinguished by calcium flux regulation during the first 10 min of lymphocyte activation. *Immunobiology* 217: 37–43, 2012.
61. Uno F, Sasaki J, Nishizaki M, Carboni G, Xu K, Atkinson EN, Kondo M, Minna JD, Roth JA, and Ji L. Myristoylation of the fus1 protein is required for tumor suppression in human lung cancer cells. *Cancer Res* 64: 2969–2976, 2004.
62. Uzhachenko R, Issaeva N, Boyd K, Ivanov SV, Carbone DP, and Ivanova AV. Tumour suppressor Fus1 provides a molecular link between inflammatory response and mitochondrial homeostasis. *J Pathol* 227: 456–469, 2012.
63. Valero RA, Senovilla L, Nunez L, and Villalobos C. The role of mitochondrial potential in control of calcium signals involved in cell proliferation. *Cell Calcium* 44: 259–269, 2008.
64. van Lent PL, Grevers LC, Blom AB, Arntz OJ, van de Loo FA, van der Kraan P, Abdollahi-Roodsaz S, Srikrishna G, Freeze H, Sloetjes A, Nacken W, Vogl T, Roth J, and van den Berg WB. Stimulation of chondrocyte-mediated cartilage destruction by S100A8 in experimental murine arthritis. *Arthritis Rheum* 58: 3776–3787, 2008.
65. Ventura-Clapier R, Garnier A, and Veksler V. Transcriptional control of mitochondrial biogenesis: the central role of PGC-1alpha. *Cardiovasc Res* 79: 208–217, 2008.
66. Waldeck-Weiermair M, Duan X, Naghdi S, Khan MJ, Trenker M, Malli R, and Graier WF. Uncoupling protein 3 adjusts mitochondrial Ca(2+) uptake to high and low Ca(2+) signals. *Cell Calcium* 48: 288–301, 2010.
67. Waldeck-Weiermair M, Jean-Quartier C, Rost R, Khan MJ, Vishnu N, Bondarenko AI, Imamura H, Malli R, and Graier WF. Leucine zipper EF hand-containing transmembrane protein 1 (Letm1) and uncoupling proteins 2 and 3 (UCP2/3) contribute to two distinct mitochondrial Ca2+ uptake pathways. *J Biol Chem* 286: 28444–28455, 2011.
68. Yap LP, Garcia JV, Han D, and Cadenas E. The energy-redox axis in aging and age-related neurodegeneration. *Adv Drug Deliv Rev* 61: 1283–1298, 2009.
69. Zozulya S and Stryer L. Calcium-myristoyl protein switch. *Proc Natl Acad Sci U S A* 89: 11569–11573, 1992.

Address correspondence to:
Dr. Alla V. Ivanova
Department of Surgery
Yale School of Medicine
333 Cedar St., BML 229
New Haven, CT 06510

E-mail: alla.ivanova@yale.edu.

Date of first submission to ARS Central, May 28, 2013; date of final revised submission, December 6, 2013; date of acceptance, December 12, 2013.

Abbreviations Used

Ca^{2+} = calcium
cyto = cytoplasmic
DAF-FM = 4-amino-5-methylamino-2′,7′-difluorofluorescein diacetate
Fluo-3/AM = fluoro-3 acetoxymethyl ester
GSH = nonprotein thiols including glutathione
IO = ionomycin
KO = knockout
MCU = mitochondrial calcium uniporter
mito = mitochondrial
MMP or $\Delta\mu H^+$ = mitochondrial membrane potential
mNCX = mitochondrial sodium–calcium exchanger
mPTP = mitochondrial permeability transition pore
Na^+ = sodium
NO = nitric oxide
ROS = reactive oxygen species
SLE = systemic lupus erythematosus
WT = wild type